PRAMANA
— journal of
physics

Vol. 86, No. 2
February 2016
pp. 343–351

A two-component dark matter model with real singlet scalars confronting GeV γ-ray excess from galactic centre and Fermi bubble

DEBASISH MAJUMDAR[1,*], KAMAKSHYA PRASAD MODAK[1] and SUBHENDU RAKSHIT[2]

[1]Astroparticle Physics and Cosmology Division, Saha Institute of Nuclear Physics, 1/AF Bidhannagar, Kolkata 700 064, India
[2]Discipline of Physics, Indian Institute of Technology Indore, IET-DAVV Campus, Indore 452 017, India
*Corresponding author. E-mail: debasish.majumdar@saha.ac.in

DOI: 10.1007/s12043-015-1154-x; ***e*Publication:** 5 January 2016

Abstract. We propose a two-component dark matter (DM) model, each component of which is a real singlet scalar, to explain results from both direct and indirect detection experiments. We put the constraints on the model parameters from theoretical bounds, PLANCK relic density results and direct DM experiments. The γ-ray flux is computed from DM annihilation in this framework and is then compared with the Fermi-LAT observations from galactic centre region and Fermi bubble.

Keywords. Two-component dark matter; galactic centre γ-ray; Fermi-LAT; Fermi bubble.

PACS No. 95.35.+d

1. Introduction

It is now established that most of the matter content of the Universe consists of unknown mysterious matter called dark matter (DM). The PLANCK observation [1] of the anisotropies in cosmic microwave background radiation (CMBR) estimates that $\sim$26.8% of the Universe consists of this DM, while only $\sim$4.9% is the known matter. This relic density of DM indicates that the DM may be composed of weakly interacting mass particles (WIMPs).

While the evidence of DM in the Universe is by and large gravitational, its particle nature is yet unknown. We propose a two-component model in this work, where the Standard Model (SM) scalar sector is extended by introducing two real gauge singlet scalars S and S'. A $\mathbb{Z}_2 \times \mathbb{Z}_2'$ symmetry is imposed on the newly added scalars to assure their stability and to qualify them for being the DM candidates. Under $\mathbb{Z}_2 \times \mathbb{Z}_2'$ symmetry,

the charge of the scalar S is $\{-1, 1\}$ and that of the other scalar S' is $\{1, -1\}$. All other SM particles are even under the symmetry. The model parameters are constrained by the theoretical bounds and PLANCK [1] relic density results. They are further constrained by DM direct detection experimental bounds.

Besides direct searches, there are experiments for indirect searches of dark matter. The dark matter particles in the Universe can be trapped by the gravity of highly gravitating astrophysical bodies such as galactic centre (GC), solar core etc. The dark matter particle undergoes scattering interactions with the other particles present in sites like GC. In this process they lose their velocities. If their velocities fall short of their escape velocities they become trapped inside these bodies. When accumulated in considerable number they may undergo self-annihilation to produce fermion–antifermion pairs, γ-rays etc., and can produce excess signal of photons or fermions–antifermions in a suitable detector. The satellite-borne experiment Fermi-LAT [2] has observed such γ-ray excess for the γ-rays from the direction of galactic centre which could not be explained from other astrophysical phenomena. The γ-ray observed by the Fermi-LAT from the GC region (5° surrounding the GC) shows a 'bumpy' structure in the photon spectrum in $\sim$10 GeV energy [3,4]. The γ-ray from other possible astrophysical sources like point source emission and galactic ridge emission cannot solely quantify this excess or 'bump' in the spectrum. One needs to add extra contribution to explain this excess. It is conjectured that the γ-rays originating from the possible DM annihilation at the GC may contribute to the observed signal. With our present formalism of two-component DM we calculate the γ-ray flux due to DM annihilation and add this contribution to those from point source and galactic ridge emissions to explain this excess. The Fermi-LAT also observed such gamma excess from the region of the Fermi bubble [5]. Fermi bubble is a bilobular structure that originates from the galactic centre and extends up to 10 kpc, perpendicular to each side of the galactic plane. An excess of γ-rays in the GeV range is found from the low-latitude regions of the Fermi bubble. We calculate the γ-ray flux from Fermi bubble region in our framework of two-singlet dark matter model.

2. Theoretical framework

In the present work, the dark matter candidate has two components S and S' both of which are real singlet scalars. The stability of S and S' are ensured by imposing a discrete symmetry, namely $Z_2 \times Z_2'$ such that $S \xrightarrow{\mathbb{Z}_2} -S$ and $S' \xrightarrow{\mathbb{Z}_2'} -S'$. Also both of them do not generate any vacuum expectation value (VEV) upon spontaneous symmetry breaking ($\langle S\rangle = 0$ and $\langle S'\rangle = 0$).

The scalar sector potential (for Higgs and two real singlet scalars) in this framework can then be written as

$$V(H, S, S') = \frac{m^2}{2}H^\dagger H + \frac{\lambda}{4}(H^\dagger H)^2 + \frac{\delta_2}{2}H^\dagger H S^2 + \frac{k_2}{2}S^2 + \frac{k_4}{4}S^4 + \frac{\delta_2'}{2}H^\dagger H S'^2 + \frac{k_2'}{2}S'^2 + \frac{k_4'}{4}S'^4 + \frac{1}{4}k_4^a SSS'S'. \quad (1)$$

After spontaneous symmetry breaking, the respective masses of S and S' are given by

$$M_S^2 = k_2 + \frac{\delta_2 v^2}{2}, \quad M_{S'}^2 = k_2' + \frac{\delta_2' v^2}{2}, \tag{2}$$

where v is VEV of the Higgs field H ($v \approx 246$ GeV). The four beyond SM parameters determining the masses of the scalars are k_2, k_2', δ_2 and δ_2'.

Model parameters can be constrained from theoretical considerations as well as from the observational and experimental results. The bounds from the theoretical considerations are listed below.

(1) *Vacuum stability conditions*

$$\lambda \geqslant 0, \quad k_4 \geqslant 0, \quad k_4' \geqslant 0, \quad \delta_2 + \sqrt{\lambda k_4} \geqslant 0, \quad \delta_2' + \sqrt{\lambda k_4'} \geqslant 0, \quad k_4^a + \sqrt{k_4 k_4'} \geqslant 0,$$
$$\sqrt{\lambda k_4 k_4'} + \delta_2 \sqrt{k_4'} + \delta_2' \sqrt{k_4} + 2k_4' \sqrt{\lambda}$$
$$+ \sqrt{(\delta_2 + \sqrt{\lambda k_4})(\delta_2' + \sqrt{\lambda k_4'})(k_4^a + \sqrt{k_4 k_4'})} \geqslant 0.$$

(2) *Perturbative unitarity bounds*

$$M_H \leq \sqrt{\frac{8\pi}{3}} v, \quad |\delta_2| \leq 8\pi, \quad |k_4| \leq \frac{8}{6}\pi, \quad |k_4'| \leq \frac{8}{6}\pi, \quad |k_4^a| \leq 8\pi, \quad |\delta_2'| \leq 8\pi.$$

(3) *Triviality bound*
We have solved all the renormalized group evolution equations in this two-singlet scalar model and checked the consistency of the quartic couplings in this model up to the suitably chosen scale of the theory.

(4) *Constraints from invisible Higgs decay width*
The invisible decay width in this model can be written as

$$\Gamma_{\text{inv}} = \frac{v^2}{32\pi M_H} \left(\delta_2^2 \sqrt{1 - \frac{4M_S^2}{M_H^2}} + \delta_2'^2 \sqrt{1 - \frac{4M_{S'}^2}{M_H^2}} \right),$$

where M_H is the mass of Higgs. This gives a bound on the parameters of this model.

2.1 *Experimental constraints*

After imposing the theoretical constraints on the model parameters, the same are subjected to further constraints from the comparison of observational and experimental results. To this end, observational results from PLANCK experiment leading to the estimation of dark matter relic density and the direct detection experimental results are considered. From the observation of anisotropies in CMBR, the PLANCK Collaboration estimated the relic density of dark matter in the Universe to be $0.1165 < \Omega_{\text{DM}} h^2 < 0.1227$ where h is the Hubble parameter expressed in units of 100 Km/Mpc/s [1]. As our present model is a two-component dark matter model, we need to obtain the relic densities of each of the two scalars S and S' of the model such that the total relic density $\Omega_{\text{DM}}^{S+S'} = \Omega_S + \Omega_{S'}$.

In order to obtain Ω_S and $\Omega_{S'}$, one needs to solve two coupled Boltzmann equation (BE) given by

$$\frac{\mathrm{d}n_S}{\mathrm{d}t}+3Hn_S=-\langle\sigma v\rangle_{SS\to XX}(n_S^2-n_{S_{\rm eq}}^2)-\langle\sigma v\rangle_{SS\to S'S'}\left(n_S^2-\frac{n_{S_{\rm eq}}^2}{n_{S'_{\rm eq}}^2}n_{S'}^2\right), \quad (3)$$

$$\frac{\mathrm{d}n_{S'}}{\mathrm{d}t}+3Hn_{S'}=-\langle\sigma v\rangle_{S'S'\to XX}(n_{S'}^2-n_{S'_{\rm eq}}^2)-\langle\sigma v\rangle_{S'S'\to SS}\left(n_{S'}^2-\frac{n_{S'_{\rm eq}}^2}{n_{S_{\rm eq}}^2}n_S^2\right). \quad (4)$$

In the above, X denotes the SM particles, H is the Hubble parameter and the subscript 'eq' denotes 'equilibrium'. Solving the coupled Boltzmann equations (eqs (3) and (4)) after computing the annihilation cross-sections $\langle\sigma v\rangle$, one obtains the corresponding abundance ($Y_0 = n/s$, where s is the entropy density and n is the number density) at the present epoch, the relic abundance of each of the components is obtained from the relation [6],

$$\Omega_S h^2 = 2.755\times10^8\left(\frac{M_S}{\rm GeV}\right)Y_0. \quad (5)$$

We have calculated the relic density and other dark matter observables using `micrOMEGAs` [7,8] code.

3. Constraining the parameter space

A direct detection experiment of dark matter particles is based on the principle that a dark matter particle scatters off a detector nucleus as a result of which the nucleus recoils with an energy ∼few keV. The scattering cross-section for the singlet scalar dark matter considered (S or S') in this model and the nucleon is given by [9]

$$\sigma^{\rm SI}_{\rm nucleon} = (\delta_2)^2\left(\frac{100\ {\rm GeV}}{M_H\ ({\rm in\ GeV})}\right)^4\left(\frac{50\ {\rm GeV}}{M_S\ ({\rm in\ GeV})}\right)^2(5\times10^{-42}\ {\rm cm}^2). \quad (6)$$

In this work we obtain the allowed values of model parameters (δ_2, δ_2', M_S and M_S') using three direct detection experiments namely CDMS II [10,11], CRESST II [12] and XENON 100 [13,14]. Needless to mention that these allowed values are obtained by simultaneously satisfying the PLANCK relic density results and other constraints described above.

The benchmark points from three dark matter direct detection experiments, namely, CDMS II, CRESS II and XENON 100 and the calculated values of scattering and annihilation cross-sections are tabulated in table 1. In figure 1, we show the allowed regions of the parameter space from the direct searches and PLANCK data. In each plot of figure 1, the bigger contour denotes the allowed region in M_S–δ_2 (or $M_{S'}$–$\delta_{2'}$) parameter space. The smaller region in the bigger contour in each plot of figure 1 is obtained when a set of parameters in the $M_S-\delta_2$ plane (benchmark point) is chosen from the allowed region (bigger contour) for the component S and then the allowed region for $M_{S'}$–$\delta_{2'}$ is found out for the other component S'.

Table 1. Benchmark points (BP) consistent with CDMS II, CRESST II, XENON 100 direct detection results and PLANCK data.

	M_S (or $M_{S'}$) (GeV)	δ_2 (or δ_2')	$\sigma^{\rm SI}$ (10^{-41} cm^2)	$\langle\sigma v\rangle$ (10^{-26} cm^3/s)		Annihilation branching fraction for S (or S') (%)
CDMS II BP	8.6	0.45	1.9	3.2	2.6 ($b\bar{b}$)	81
					0.4 ($c\bar{c}$)	12
					0.2 ($l\bar{l}$)	7
	6.7	0.82	9.9	8.3	6.3 ($b\bar{b}$)	77
					1.2 ($c\bar{c}$)	15
					7.2 ($l\bar{l}$)	8
CRESST II BP	25.3	0.36	1.6	3.0	2.4 ($b\bar{b}$)	81
					0.4 ($c\bar{c}$)	12
					0.2 ($l\bar{l}$)	7
	23.3	0.47	3.2	4.8	3.9 ($b\bar{b}$)	81
					0.6 ($c\bar{c}$)	12
					0.3 ($l\bar{l}$)	7
XENON 100 BP	90.0	0.050	2.6	4.32	4.29 (W^+W^-)	99.3
					0.024 ($b\bar{b}$)	0.55
					0.004 ($c\bar{c}$)	0.10
					0.002 ($l\bar{l}$)	0.05
	92.0	0.045	2.0	3.78	3.28 (W^+W^-)	86.6
					0.48 (ZZ)	12.8
					0.016 ($b\bar{b}$)	0.43
					0.003 ($c\bar{c}$)	0.08
					0.002 ($l\bar{l}$)	0.05

4. Confronting calculated γ-ray with Fermi-LAT results for galactic centre region

The differential flux of γ-ray due to dark matter annihilation in galactic halo in angular direction that produce a solid angle $\Delta\Omega$ is given by [15]

$$\frac{{\rm d}\Phi_\gamma}{{\rm d}E_\gamma} = \frac{1}{8\pi}\sum_f \frac{\langle\sigma v\rangle_f}{M_{S,S'}^2}\frac{{\rm d}N_\gamma^f}{{\rm d}E_\gamma} r_\odot \rho_\odot^2 \bar{J}\Delta\Omega, \quad J = \int_{l.o.s}\frac{{\rm d}s}{r_\odot}\left(\frac{\rho(r)}{\rho_\odot}\right)^2. \tag{7}$$

In the above, the γ-ray spectrum is given by the term ${\rm d}N_\gamma^f/{\rm d}E_\gamma$ where f denotes the final-state fermions $f\bar{f}$ from dark matter annihilation $SS \to f\bar{f}$ and J is the astrophysical J-factor defined above. Also

$$\bar{J} = \frac{4}{\Delta\Omega}\int {\rm d}\ell \int {\rm d}b\, \cos b\, J(\ell, b) \quad (\ell, b \ \text{coordinate}). \tag{8}$$

In the above $\rho(r)$ denotes the DM halo profile.

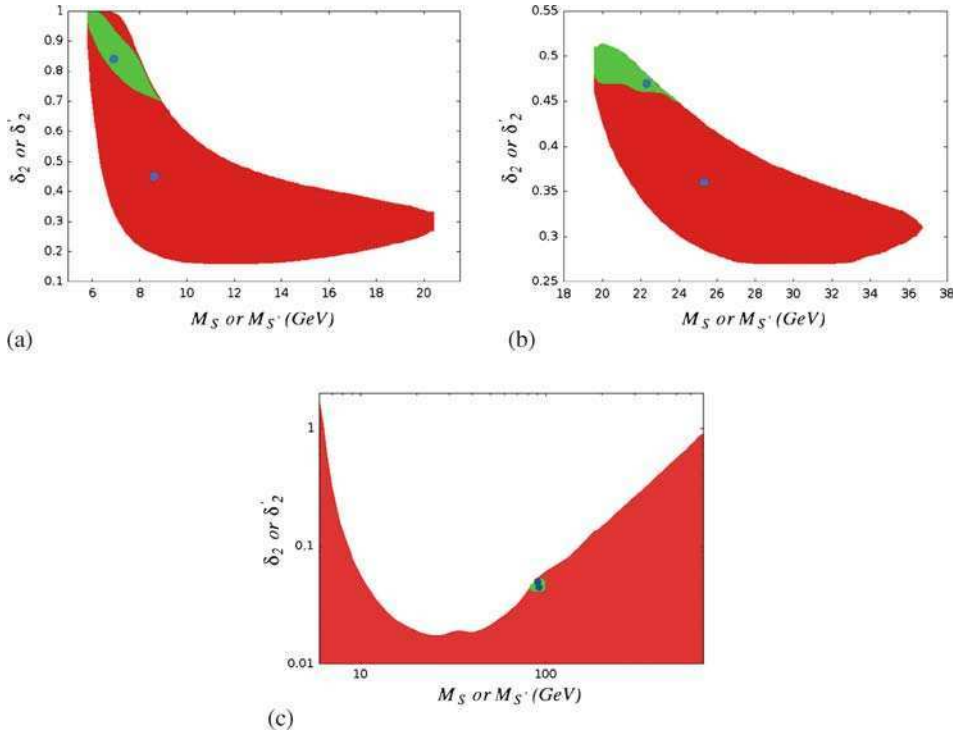

Figure 1. The allowed parameter space constrained by DM direct detection experimental results and PLANCK data for DM relic density. We show the results for three chosen benchmark points of table 1 considering (**a**) CDMS II, (**b**) CRESST II and (**c**) XENON 100 direct DM search experiments. The red region in each plot is the allowed parameter space by direct detection experiment for any singlet S ($M_S - \delta_2$) or S' ($M'_S - \delta'_2$), while the green region in each plot denotes the allowed parameter space satisfied by PLANCK for any of the singlets S or S' when the parameters for the other singlet are fixed. The two blue dots in each plot denote the chosen benchmark point. See text for details.

The radial distance r from GC can be expressed in terms of the distance s along the line of sight and the galactic coordinates ℓ and b as

$$r = \left(s^2 + r_\odot^2 - 2sr_\odot \cos\ell\cos b\right)^{1/2} \quad (\ell, b \text{ coordinate}). \tag{9}$$

In the numerical calculation of the gamma flux, the local dark matter density $\rho_\odot$ is taken to be 0.4 GeV/cm^3 and the distance between Sun and GC, $r_\odot = 8.5$ kpc. $\rho(r)$ is given in the following form:

$$\rho(r) = \frac{\rho_\odot}{(r/r_c)^\gamma [1 + (r/r_c)^\gamma]^{(\beta-\gamma)/\alpha}}, \tag{10}$$

where α, β, γ and r_c are the parameters where $\{\alpha, \beta, \gamma, r_c(\text{kpc})\} = \{1, 3, 1, 20\}$ (NFW profile) [16,17], $\{1.5, 3, 1.5, 28\}$ (Moore profile) [18], $\{2, 2, 0, 3.5\}$ (isothermal profile) [19]. Another different halo profile called Einasto profile [20] is also considered in our calculations.

Using eqs (7)–(10), we compute the γ-ray flux for the benchmark points given in table 1 for all the chosen halo profiles. We then add to this computed flux the contribution from

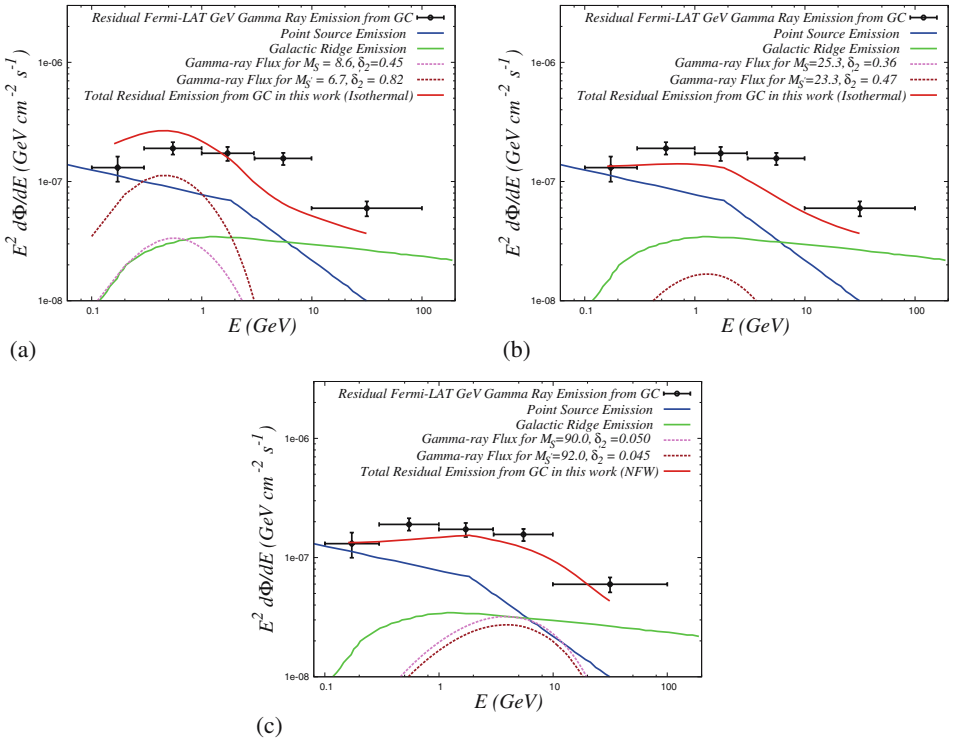

Figure 2. The residual γ-ray flux from inner 5° from GC and its comparison with the Fermi-LAT results. Calculations are made with the benchmark point corresponding to (**a**) CDMS II bounds and isothermal halo profile, (**b**) CRESST II bounds and isothermal halo profile, (**c**) XENON 100 bounds and NFW halo profile. See text for details.

the point source emission as well as the galactic ridge emission. We then compute total gamma flux using each of the profiles mentioned earlier and compare each of them with the Fermi-LAT results. In figure 2, we show the results corresponding to those profiles that describe best the observed data.

5. The γ-ray excess from Fermi bubble region

The Fermi bubble [5] which is a lobular structure that originates at the galactic centre and extends upto ∼50° (∼10 kpc) on both sides perpendicular to the GC has been found to emit γ-rays (Fermi-LAT observation) between the range of ∼few GeV and ∼100 GeV. While the gamma spectrum, from the region of the Fermi bubble which is far from the galactic plane, follows a power law $\sim E^{-2}$, gamma from the region nearer to the galactic plane cannot be explained solely by a power law form. While the observed γ-rays from higher galactic latitude region of the bubble can be explained by processes like inverse Compton scattering of the high-energy electrons, those from the lower latitude region of the bubble cannot be fully explained by known astrophysical processes [21–23]. As the DM density is expected to be high for regions close to GC, we calculate the contribution

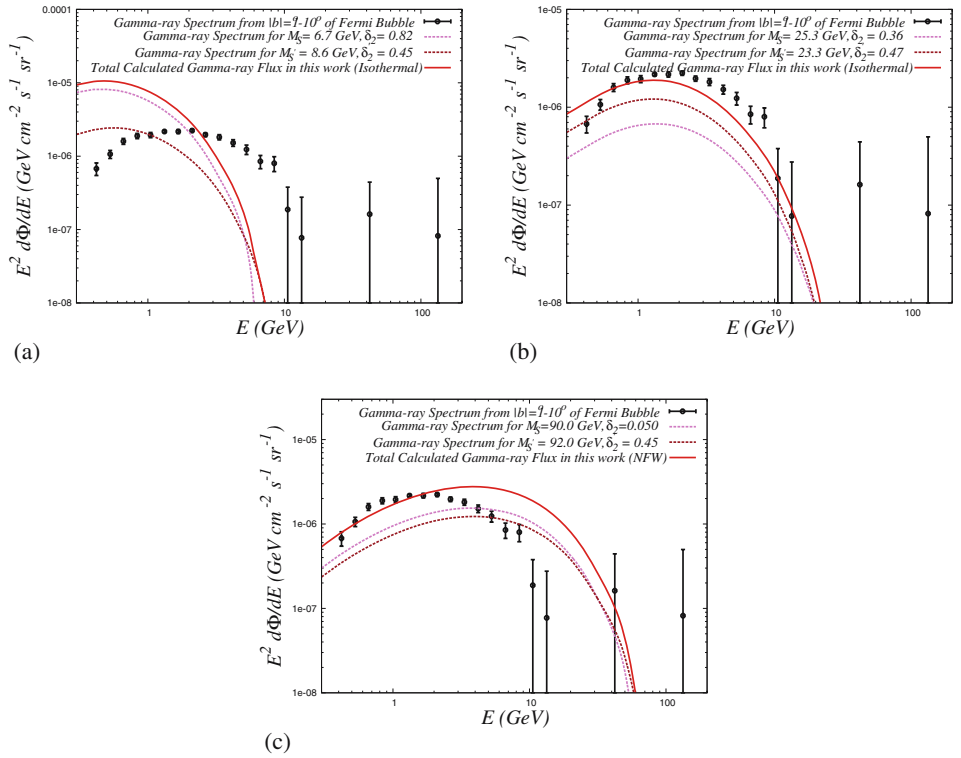

Figure 3. Comparison of calculated γ-ray flux with the γ-ray emission spectrum from the low-latitude ($|b| = 1°–10°$) region of the Fermi bubble. Black points are the observed data after subtracting the inverse Compton scattering contribution of the high-energy electrons. In each plot, the contribution from the pair annihilation of singlet S is shown by the pink dashed line whereas that from the pair annihilation of singlet S' is shown by the brown dashed line. The total contribution coming from DM (both S and S') annihilations in this model is shown by the solid red line in each plot. Each plot in this figure is for a different benchmark point with a DM halo profile which explains GC low energy γ-ray 'bump' very well. See text for details.

of annihilating dark matter in the framework of our present model to explain the observed γ-ray spectrum from lower latitude ($\sim$1°–10°) region of the Fermi bubble.

In figure 3, we present our results for the benchmark points described above and compare them with the observational results. In doing this, we have chosen those benchmark points (and the density profiles) that yield best agreements for the galactic centre γ-ray excesses (§4). It is also seen from our study that the isothermal profile (flat profile) appears to be a better choice for the DM in the low mass range ($\sim$10 GeV), while NFW profile (cuspy profile) is more suited for higher mass DM particles.

6. Discussions

For the two-component scalar singlet DM that is considered in this work, the stability of DM is ensured by imposing a $\mathbb{Z}_2 \times \mathbb{Z}_2'$ symmetry. We constrained the DM model parameter

space from theoretical conditions as well as PLANCK results for DM relic density. They are further restricted by the direct detection experimental results. We solve the coupled BE for obtaining the DM relic density in this model. We calculate the DM annihilation cross-sections and compute the γ-ray flux from GC region and Fermi bubble for various halo profiles. They are then compared with the Fermi-LAT γ-ray observational results for both the galactic centre region and the Fermi bubble. We conclude that our model can confront reasonably well the low-energy γ-ray excess from galactic centre as well as from the low latitude of Fermi bubble.

References

[1] PLANCK Collaboration: P A R Ade *et al*, *Astron. Astrophys.* **571**, A16 (2014), arXiv:1303.5076 [astro-ph.CO]
[2] Fermi/LAT Collaboration: W B Atwood *et al*, *Astrophys. J.* **697**, 1071 (2009), arXiv:0902.1089 [astro-ph.IM]
[3] D Hooper and L Goodenough, *Phys. Lett. B* **697**, 412 (2011)
[4] A Boyarsky, D Malyshev and O Ruchayskiy, *Phys. Lett. B* **705**, 165 (2011)
[5] M Su, T R Slatyer and D P Finkbeiner, *Astrophys. J.* **724**, 1044 (2010), arXiv:1005.5480 [astro-ph.HE]
[6] J Edsjö and P Gondolo, *Phys. Rev. D* **56**, 1879 (1997)
[7] G Belanger, F Boudjema, P Brun, A Pukhov, S Rosier-Lees, P Salati and A Semenov, *Comput. Phys. Commun.* **182**, 842 (2011), arXiv:1004.1092 [hep-ph]
[8] G Belanger, F Boudjema, A Pukhov and A Semenov arXiv:1305.0237 [hep-ph]
[9] C P Burgess, M Pospelov and T ter Veldhuis, *Nucl. Phys.* **B619**, 709–728 (2001), hep-ph/0011335
[10] Z Ahmed *et al*, *Science* **327**, 1619 (2010)
[11] CDMS Collaboration: R Agnese *et al*, *Phys. Rev. D* **88**, 031104 (2013), arXiv:1304.3706 [astro-ph.CO]
CDMS Collaboration: R Agnese *et al*, arXiv:1304.4279 [hep-ex]
[12] G Angloher, M Bauer, I Bavykina, A Bento, C Bucci, C Ciemniak, G Deuter, F von Feilitzsch *et al*, *Eur. Phys. J. C* **72**, 1971 (2012), arXiv:1109.0702 [astro-ph.CO]
[13] XENON100 Collaboration: E Aprile *et al*, *Phys. Rev. Lett.* **107**, 131302 (2011), arXiv:1104.2549 [astro-ph.CO]
[14] XENON100 Collaboration: E Aprile *et al*, *Phys. Rev. Lett.* **109**, 181301 (2012), arXiv:1207.5988 [astro-ph.CO]
[15] M Cirelli, G Corcella, A Hektor, G Hutsi, M Kadastik, P Panci, M Raidal, F Sala *et al*, *J. Cosmol. Astorpart. Phys.* **1103**, 051 (2011)
Erratum, *ibid*. **1210**, E01 (2012), arXiv:1012.4515 [hep-ph]
[16] J F Navarro, C S Frenk and S D M White, *Astrophys. J.* **462**, 563 (1996)
[17] J F Navarro, C S Frenk and S D M White, *Astrophys. J.* **490**, 493 (1997)
[18] B Moore, T Quinn, F Governato, J Stadel and G Lake, *Mon. Not. R. Astron. Soc.* **310**, 1147 (1999)
J Diemand, B Moore and J Stadel, *Mon. Not. R. Astron. Soc.* **353**, 624 (2004)
B Moore *et al*, *Astrophys. J.* **499**, L5 (1998)
[19] J N Bahcall and R M Soneira, *Astrophys. J. Suppl.* **44**, 73 (1980)
[20] J Einasto, *Trudy Inst. Astroz. Alma-Ata* **51**, 87 (1965)
[21] W-C Huang, A Urbano and W Xue, arXiv:1307.6862 [hep-ph]
[22] W-C Huang, A Urbano and W Xue, arXiv:1310.7609 [hep-ph]
[23] D Hooper and T R Slatyer, *Phys. Dark Univ.* **2**, 118 (2013), arXiv:1302.6589 [astro-ph.HE]